Structural Engineering and Mechanics, Vol. 16, No. 2 (2003) 177-193
DOI: http://dx.doi.org/10.12989/sem.2003.16.2.177

Inserting the mass proportional damping (MPD) system in a concrete shear-type structure

Stefano Silvestri†, Tomaso Trombetti‡ and Claudio Ceccoli‡†

Department DISTART, University of Bologna, Viale Risorgimento 2, 40136 Bologna, Italy

(Received December 20, 2002, Accepted June 13, 2003)

Abstract. This paper presents an illustrative example of the advantages offered by inserting added viscous dampers into shear-type structures in accordance with a special scheme based upon the mass proportional damping (MPD) component of the Rayleigh viscous damping matrix. In previous works developed by the authors, it has been widely shown that, within the class of Rayleigh damped systems and under the "equal total cost" constraint, the MPD system provides best overall performance both in terms of minimising top-storey mean square response to a white noise stochastic input and maximising the weighted average of modal damping ratios. A numerical verification of the advantages offered by the application of MPD systems to a realistic structure is presented herein with reference to a 4-storey reinforced-concrete frame. The dynamic response of the frame subjected to both stochastic inputs and several recorded earthquake ground motions is here analysed in detail. The results confirm the good dissipative properties of MPD systems and indicate that this is achieved at the expense of relatively small damping forces.

Key words: added viscous dampers; concrete shear-type structure; Rayleigh damping matrix; MPD system; seismic response.

1. Introduction

Dissipative systems have widely proven their effectiveness in mitigating seismic effects in shear-type structures (Hart and Wong 2000), (http://nisee.berkeley.edu). Still the issue is open in terms of identifying the additional damper system that maximizes the overall dissipative properties of the structure under a wide range of dynamic inputs and with reference to a number of performance indexes (De Silva 1981, Constantinou and Tadjbakhsh 1983, Hahn and Sathiavageeswaran 1992, Zhang and Soong 1992, Takewaki 1997, 1998, 1999, 2000, Lopez Garcia 2001, Singh and Moreschi 2001, 2002). In previous works (Trombetti *et al.* 2001, 2002), the authors have examined the problem in an innovative, across-the-board manner by studying damper placement and sizing contemporarily. This approach has led to the identification of the optimal damping properties of the so-called MPD system (a limiting case of Rayleigh damping).

In this paper, the properties of Rayleigh damping systems are first recalled together with those of

† Ph.D. Student
‡ Assistant Professor (Researcher)
‡† Full Professor

the MPD and SPD limiting cases. Secondly, the dissipative performances of MPD systems are compared to those of generic Rayleigh damping systems through the analysis of the dynamic behaviour of a reference 4-storey reinforced-concrete frame shear-type structure.

2. Definitions and properties of MPD and SPD systems

The Rayleigh damping matrix of multi-degree-of-freedom (MDOF) systems has the following expression (Clough and Penzien 1993):

$$[C]_R = \alpha[M] + \beta[K] \tag{1}$$

where $[M]$ and $[K]$ are, respectively, the mass matrix and the stiffness matrix, and α and β are two proportionality constants having units of sec^{-1} and sec, respectively. Eq. (1) allows us to define the mass proportional damping (MPD) and stiffness proportional damping (SPD) limiting cases of Rayleigh damping respectively characterised by the following damping matrices:

$$[C]_{MPD} = \alpha[M] \tag{2}$$

$$[C]_{SPD} = \beta[K] \tag{3}$$

For the sake of clarity, in the following analysis internal (intrinsic) damping is neglected. The added-damper system which allows an MPD matrix to be obtained is defined herein as “MPD system” and, likewise, that which allows an SPD matrix to be obtained is referred to as “SPD system”. Furthermore, structures characterised by an MPD system will be indicated hereafter as “MPD structures”, whilst those featuring an SPD system will be called “SPD structures”.

MPD and SPD systems are characterised by opposite damping properties. The n-th modal damping ratios of the MPD and SPD systems (referred to herein as ξ_n^{MPD} and ξ_n^{SPD}, respectively) are defined (Clough and Penzien 1993, Chopra 1995) as follows:

$$\xi_n^{MPD}(\omega_n) = \frac{\alpha}{2\omega_n} \tag{4}$$

$$\xi_n^{SPD}(\omega_n) = \frac{\beta\omega_n}{2} \tag{5}$$

where ω_n is the n-th modal circular frequency. It is clear that ξ_n^{MPD} and ξ_n^{SPD} are, respectively, inversely and directly proportional to ω_n. Consequently, as shown in Fig. 1(a), MPD systems damp mainly in correspondence with the first modes of vibration (which are characterised by low values of circular frequency ω). On the other hand, as shown in Fig. 1(b), the dissipative efficiency of SPD systems increases in line as the number of the mode gets higher and higher.

As explained in detail in previous works (Trombetti *et al.* 2001, 2002) developed by the authors, the MPD and SPD systems correspond to physically separated and actually independently implementable damper systems. Figs. 2(a) and 2(b) represent, for an illustrative 3-storey shear-type structure, the MPD and SPD systems. In these figures and in the following, u_j denotes the displacement of the j-th storey, m_j the j-th floor mass and k_j the horizontal lateral stiffness of the vertical members which connect the $(j-1)$-th storey with the j-th one.

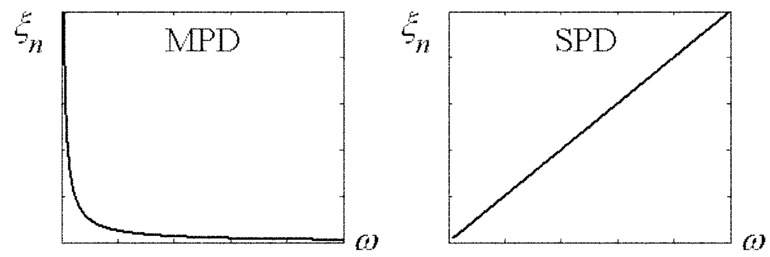

(a) (b)

Fig. 1 ξ_n vs. ω curves for (a) MPD and (b) SPD systems

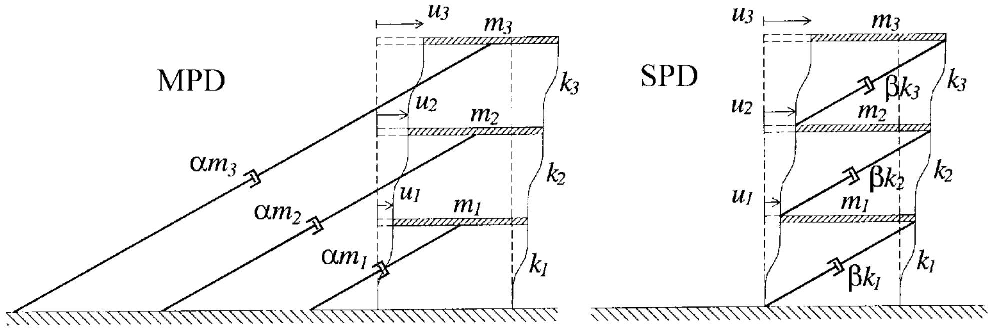

(a) (b)

Fig. 2 3-storey shear-type structure damped (a) with MPD system and (b) with SPD system

Notice that SPD systems are characterised by a damper placement (dampers positioned between adjacent storeys) that is usually adopted when implementing such dissipative systems in shear-type structures. MPD systems, on the other hand, are characterised by an innovative damping arrangement that sees dampers connecting each storey to a fixed point (MPD placement). In previous works by the authors (Trombetti *et al.* 2001, 2002), it has been pointed out that the damper placement controls the dissipative properties of the system more strongly than the damper sizing (damper sized either proportionally to the interstorey stiffness k_j or the storey mass m_j). For this reason, the comparison between the performances offered by MPD and SPD systems (provided in the following) can be seen as a comparison between the traditional interstorey damper placement and the innovative MPD placement proposed by the authors.

3. Search for the most efficient Rayleigh damping system

To identify the most efficient Rayleigh system in terms of energy dissipation among all those implementable in shear-type structures, it is necessary to:

- introduce a constraint which allows a meaningful comparison;
- define a number of performance indexes (no unique damping ratio can be defined for MDOF systems) to be optimised.

3.1 The “equal total cost” constraint

This constraint requires that the total cost of a damping system, c_{tot}, calculated as the sum of the damping coefficients, c_j, of all M dampers introduced into the structure, be equal to a set value, $\bar{c}$, for all systems considered. This is represented by the formula:

$$c_{tot} = \sum_{j=1}^{M} c_j = \bar{c} \tag{6}$$

For a generic N-d.o.f. Rayleigh system, Eq. (6) leads to:

$$\alpha \sum_{j=1}^{N} m_j + \beta \sum_{j=1}^{N} k_j = \bar{c} \tag{7}$$

which, in turn, identifies a system class characterised by the following α and β values:

$$\alpha = \bar{\alpha} \cdot (1 - \gamma) \tag{8}$$

$$\beta = \bar{\beta} \cdot \gamma \tag{9}$$

where $\bar{\alpha} = \bar{c} / \sum_{j=1}^{N} m_j$, $\bar{\beta} = \bar{c} / \sum_{j=1}^{N} k_j$ and γ is a dimensionless parameter with values ranging between 0 and 1 that identifies each specific Rayleigh system within the class defined above. $\gamma = 0$ identifies the MPD system, whilst $\gamma = 1$ identifies the SPD system.

3.2 Performance indexes adopted

The efficiency of the various damping systems is assessed herein using the following performance indexes.

Firstly, an index based upon the stochastic input response of the structure is considered. More specifically, use is made of the mean square response (Crandall and Mark 1963, Skalmierski and Tylikowski 1982, Trombetti *et al.* 2001, 2002), (that coincides with variance for stochastic inputs with zero mean value), σ_j^2, of j-th storey displacement of the structure subjected to the following base acceleration stochastic input[1]:

- stationary band-limited (between 0 and $\bar{\omega}$ = 60 rad/sec) Gaussian zero-mean white noise;
- characterised by constant power spectral density of amplitude A^2 = 0.144 m^2/sec^3.

Secondly, an index based upon the modal damping ratios of the damped structure is taken into consideration. More specifically, the modal damping ratio weighted average, ξ_{av}^R (where subscript *av* stands for *average*), is computed as:

$$\xi_{av}^R = \sum_{n=1}^{N} \bar{V}_{bn} \xi_n^R \tag{10}$$

[1]The characteristics of the stochastic process have been chosen so that its standard deviation is equal to 0.3 g, being g the acceleration of gravity.

where ξ_n^R is the n-th modal damping ratio of the generic Rayleigh system (Clough and Penzien 1993):

$$\xi_n^R = \frac{\alpha}{2\omega_n} + \frac{\beta\omega_n}{2} \tag{11}$$

and the weights $\bar{V}_{bn}$ are the base shear *modal contribution factors*, as defined by Chopra (1995):

$$\bar{V}_{bn} = \frac{M_n^*}{\sum_{n=1}^{N} M_n^*} \tag{12}$$

where M_n^* represents the *base shear effective modal mass* (Chopra 1995, Trombetti *et al.* 2002) of the structure's n-th mode of vibration.

From Eqs. (4), (5), (10) and (11) and by imposing the "equal total cost" constraint provided by Eqs. (8) and (9), the modal damping ratio weighted averages for MPD, ξ_{av}^{MPD}, and SPD, ξ_{av}^{SPD}, and generic Rayleigh damping, ξ_{av}^{R}, systems are computed as follows:

$$\xi_{av}^{MPD} = \sum_{n=1}^{N} \bar{V}_{bn} \frac{\bar{\alpha}}{2\omega_n} \tag{13}$$

$$\xi_{av}^{SPD} = \sum_{n=1}^{N} \bar{V}_{bn} \frac{\bar{\beta}\omega_n}{2} \tag{14}$$

$$\xi_{av}^{R} = (\xi_{av}^{SPD} - \xi_{av}^{MPD})\gamma + \xi_{av}^{MPD} \tag{15}$$

Finally, the maximum values of a number of structural response parameter time histories are studied and compared to assess the dissipative effectiveness of Rayleigh damped structures when subjected to a wide set of recorded earthquake ground motions.

4. Reference 4-storey r.c. frame structure

As a realistic example, let us consider a reinforced concrete (r.c.) residential building designed in a class II seismic zone, as defined by Italian Ministerial Decree 16/1/1996.

The reference structure has a rectangular layout of 19 m × 11.3 m and measures 10.42 m at its highest point. The gable roof has a pitch of around 15%. The structure consists of three frames, two lateral and one central, arranged lengthways along the building plan (19 m) and connected by r.c. beams of sufficient size to provide earthquake resistance. The slabs are arranged crosswise with a gap of 5.65 m. The building has no basement, the 1st floor is used as office space and the 2nd as living accommodation. Inter-storey height is 3 m. The 3rd floor is uninhabitable and considered an attic with height varying from zero to 1.42 m at the centre. The roof represents the 4th floor.

In the analysis presented herein, the central frame is considered separate from the rest of the system. Fig. 3(a) shows the formwork of this frame. Fig. 3(b) shows the frame's two-dimensional shear-type schematisation used to study its dynamic behaviour. Storey stiffness values, k_j, have been calculated using a two-dimensional finite element model that takes account of the finite stiffness of the beams. The resultant stiffness values are set out here below:

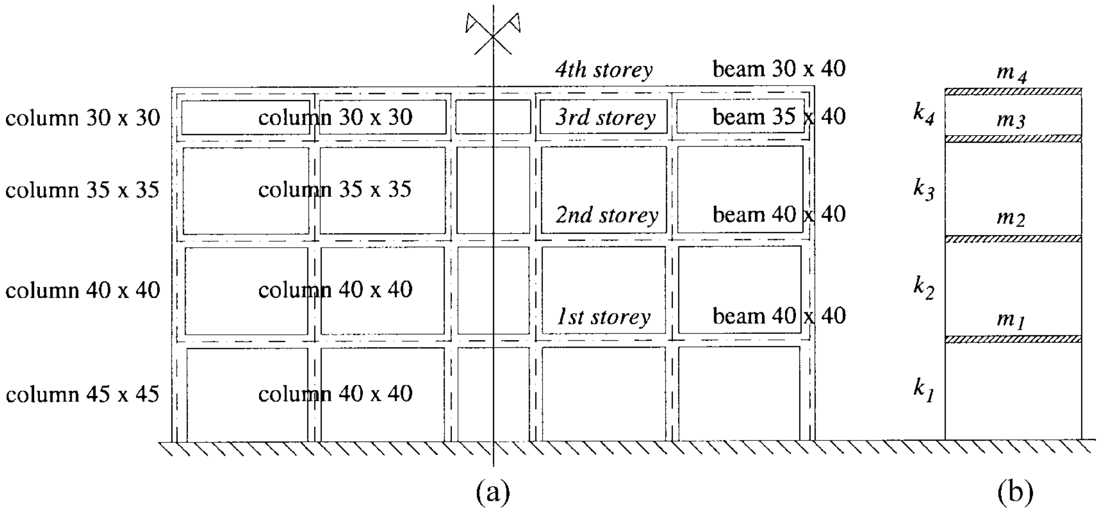

Fig. 3 (a) Central-frame formwork, (b) Shear-type schematisation of central frame

$$\begin{aligned} k_1 &= 1.000 \cdot 10^8 \text{ N/m} \\ k_2 &= 0.601 \cdot 10^8 \text{ N/m} \\ k_3 &= 0.435 \cdot 10^8 \text{ N/m} \\ k_4 &= 1.278 \cdot 10^8 \text{ N/m} \end{aligned} \tag{16}$$

Storey masses have been calculated according to the provisions of Italian Ministerial Decree 16/1/1996 and take into account different live loads according to the use of each floor:

$$\begin{aligned} m_1 &= 1.03 \cdot 10^5 \text{ kg} \\ m_2 &= 0.93 \cdot 10^5 \text{ kg} \\ m_3 &= 0.78 \cdot 10^5 \text{ kg} \\ m_4 &= 0.60 \cdot 10^5 \text{ kg} \end{aligned} \tag{17}$$

As previously stated, the system is assumed to have no internal damping. The additional damping systems analysed in the following are characterised by $\bar{c} = 3.117 \cdot 10^6$ N · sec/m (this leads to $\xi_1^{SPD} = 0.05$).

5. Numerical results

This section investigates the dependence of the dynamic performances of the above-defined frame upon the characteristics of the added viscous damper systems. Only systems leading to Rayleigh damping matrices are here taken into account. The dynamic performances of the structure equipped with such damping systems are presented first with respect to overall indexes derived from the system dynamic properties (5.1 and 5.2) and then with respect to the specific dynamic response of the system to selected earthquake inputs (5.3).

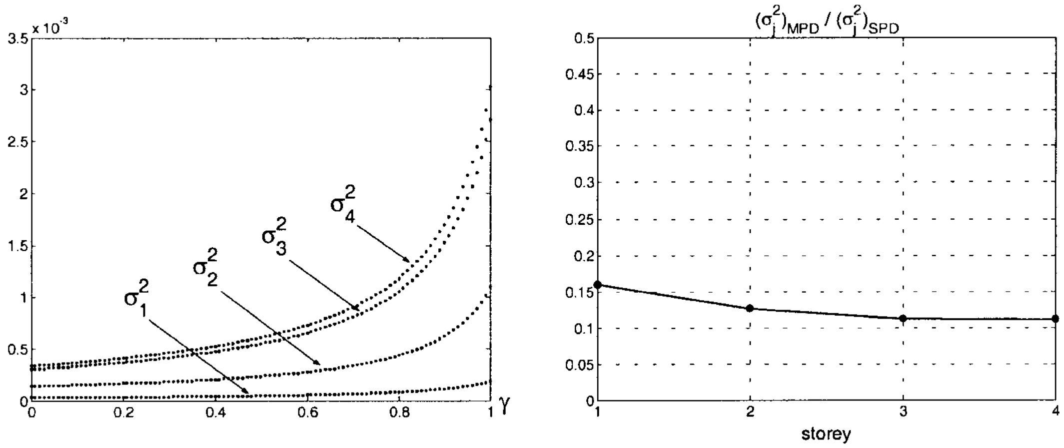

(a) (b)

Fig. 4 (a) Values of index σ_j^2, for each storey *j*, as a function of γ, (b) Ratio $(\sigma_j^2)_{MPD}/(\sigma_j^2)_{SPD}$ for each storey *j*

5.1 Storey mean square response to stochastic input

Fig. 4(a) represents, for each *j*-th storey, the mean square response σ_j^2 to the stochastic input defined in section 3.2, as a function of γ. Parameter γ identifying each specific Rayleigh damping system within the class defined by Eqs. (8) and (9). It is immediately noticeable how the MPD system ($\gamma = 0$) minimises the mean square response σ_j^2, for every storey, whilst the SPD system ($\gamma = 1$) maximises it.

Fig. 4(b) represents the ratio $(\sigma_j^2)_{MPD}/(\sigma_j^2)_{SPD}$ for each *j*-th storey. Mean square responses $(\sigma_j^2)_{MPD}$ and $(\sigma_j^2)_{SPD}$ indicating, respectively, the values of σ_j^2 calculated for $\gamma = 0$ and $\gamma = 1$.

Fig. 4(a) allows the following additional observations to be made:

- all curves are extremely smooth and characterised by a virtually horizontal tangent at $\gamma = 0$. This indicates an exceptional “robustness” of the MPD system’s dissipation efficiency;
- the $\sigma_3^2(\gamma)$ and $\sigma_4^2(\gamma)$ curves show a cusp with an almost vertical tangent at $\gamma = 1$. This fact clearly indicates that high values for $\sigma_3^2(\gamma)$ and $\sigma_4^2(\gamma)$ are closely linked with “pure” SPD systems (γ exactly equal to 1). If seeking high dissipation efficiency, SPD systems should be avoided at all costs. These two curves are very tight. This can be explained by the relatively high value of the stiffness (k_4) of the vertical members connecting the 3rd and 4th floors (due to the lowness of the attic). To all intents and purposes, the structure behaves as though it had just three storeys, since the 3rd and 4th floors constitute an extremely stiff single body;
- as one might expect, for each given γ value, σ_j^2 increases as the storey number becomes higher. Nevertheless, MPD systems produce σ_j^2 values that are much lower and similar to each other for all four storeys. SPD systems produce extremely different σ_j^2 values, so that $(\sigma_4^2)_{SPD} \cong 16 \cdot (\sigma_1^2)_{SPD}$ and $(\sigma_4^2)_{SPD} \cong 2.75 \cdot (\sigma_2^2)_{SPD}$;
- the absolute difference between $(\sigma_j^2)_{MPD}$ and $(\sigma_j^2)_{SPD}$ increases as the storey number *j* becomes higher.

Fig. 4(b) allows a quantitative assessment of the reduction in σ_j^2 of the MPD system, as compared to the values of the same index of the SPD system, under the “equal total cost” constraint. It can be seen that the ratio $(\sigma_j^2)_{MPD}/(\sigma_j^2)_{SPD}$ is roughly constant for all storeys. More in detail:

- for the 1st storey, the MPD system reduces the σ_1^2 value obtained with the SPD system by about 84%;
- for the 2nd storey, the MPD system reduces the σ_2^2 value obtained with the SPD system by about 87%;
- for the 3rd and 4th storey, the MPD system reduces the σ_3^2 and σ_4^2 values obtained with the SPD system by about 89%.

5.2 Modal damping ratio weighted average

From Eqs. (13) and (14): $\xi_{av}^{MPD} = 0.385$ and $\xi_{av}^{SPD} = 0.069$, this indicates that the MPD system is characterised by an "equivalent" damping ratio which is about five times larger than that of the SPD system. From Eq. (15) it is clear that ξ_{av}^{R} of any Rayleigh damping system is bounded between the above values.

5.3 Response to earthquake ground motions

In order to crosscheck the validity of the above-mentioned results, a series of numerical simulations are conducted using as inputs 40 historically recorded earthquake ground motions (10 near-field and 30 far-field).

The damping systems characterised by $\gamma = 0$ (MPD system), $\gamma = 1$ (SPD system) and $\gamma = 0.5$ are taken into consideration. All systems are characterised, as before, by total cost $\bar{c} = 3.117 \cdot 10^6$ N · sec/m. For the sake of clarity, hereinafter, reference will be made to MPD ($\gamma = 0$), SPD ($\gamma = 1$) and R05 ($\gamma = 0.5$) systems/structures, respectively.

By taking the maximum displacement developed by the SPD structure as a reference, the following two ratios $(\rho_j)_{MPD}$ and $(\rho_j)_{R05}$ are calculated for each of the four storeys and for each earthquake input:

$$(\rho_j)_{MPD} = \frac{(u_{\max-j})_{MPD}}{(u_{\max-j})_{SPD}} \tag{18}$$

$$(\rho_j)_{R05} = \frac{(u_{\max-j})_{R05}}{(u_{\max-j})_{SPD}} \tag{19}$$

where $(u_{\max-j})_{MPD}$, $(u_{\max-j})_{SPD}$, $(u_{\max-j})_{R05}$ represent, respectively, the maximum displacement of the j-th storey developed by MPD, SPD and R05 structures.

The above ratios indicate, respectively, the reduction in the maximum displacement offered by MPD and R05 structures compared to the maximum displacement developed by the SPD structure at the j-th storey.

For each j-th storey, the average and standard deviations of the two ratios $(\rho_j)_{MPD}$ and $(\rho_j)_{R05}$, calculated for a given earthquake population, are indicated hereafter as $\mu_{\rho MPD}$, $\sigma_{\rho MPD}$, $\mu_{\rho R05}$ and $\sigma_{\rho R05}$, respectively. The graphs shown in Figs. 5(a), 5(b) and 5(c) represent, respectively, $\mu_{\rho MPD}$, $\mu_{\rho MPD} \pm \sigma_{\rho MPD}$, $\mu_{\rho R05}$ and $\mu_{\rho R05} \pm \sigma_{\rho R05}$ for the population of 30 far-field earthquakes only, the population of 10 near-field earthquakes only and the entire population of all 40 earthquakes considered. All graphs provide the same indications: both MPD and R05 systems are capable of providing a sizable reduction in maximum storey displacements with reference to those developed by the structure equipped with SPD system. The values of $\mu_{\rho MPD}$ and $\mu_{\rho R05}$ are in fact in all cases well below unity.

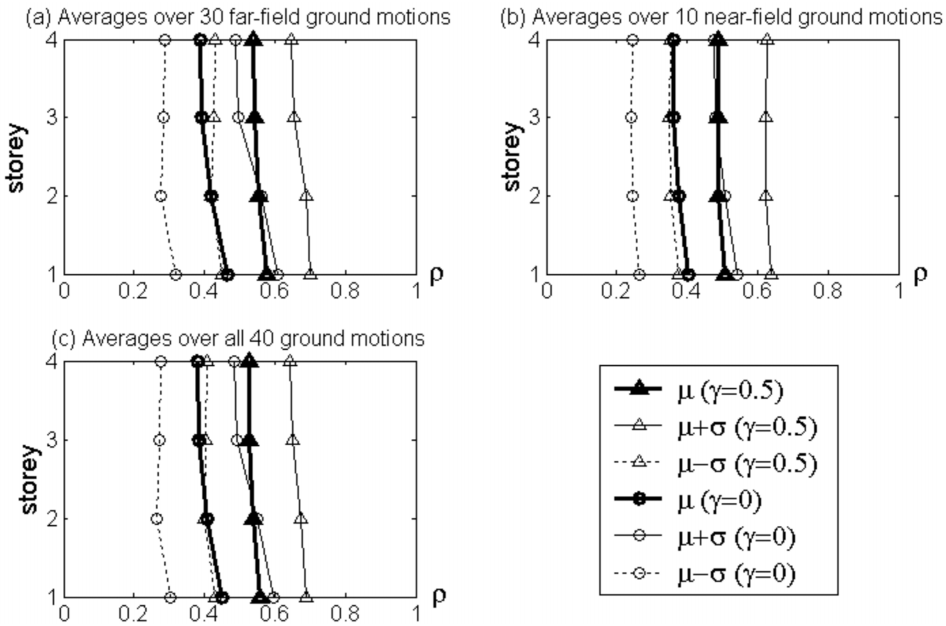

Fig. 5 $\mu_{\rho MPD}$, $\mu_{\rho MPD} \pm \sigma_{\rho MPD}$, $\mu_{\rho R05}$ and $\mu_{\rho R05} \pm \sigma_{\rho R05}$ (a) for the population of 30 far-field earthquakes only, (b) the population of 10 near-field earthquakes only and (c) the entire population of all 40 earthquakes considered

In detail:

- the MPD system provides an average reduction in maximum storey displacement of 55% on the 1st floor, 59% on the 2nd floor and 62% on the 3rd and 4th floor;
- the R05 system provides slightly smaller reduction: 44% on the 1st floor, 46% on the 2nd floor and 47% on the 3rd and 4th floor;
- in both above cases, displacement reduction is more marked on the higher floors, with $\mu_{\rho MPD}$ and $\mu_{\rho R05}$ showing a progressive increase from the top to the bottom of the structure.

The "relative" proximity between the two curves representing $\mu_{\rho MPD}$ and $\mu_{\rho R05}$ (with respect to reference value 1) is indicative of the fact that it is sufficient to provide the structure at each storey with ground-connected dampers, even of limited size (i.e., which do not reach the full mass proportional value), in order to achieve a notable reduction in the structure's maximum displacement.

In addition to the above analysis regarding the maximum storey displacements, also the maximum values of floor accelerations, interstorey drift angles, storey shears and damper forces developed by the MPD, SPD and R05 systems are evaluated for the same 40 seismic excitations considered before.

Figs. 6-8 show selected results obtained for the following earthquake ground motion records:

- Imperial Valley, 1940, El Centro record, NS component (270^{o}), PGA = 0.215 g;
- Kern County, 1952, Taft Lincoln School record, EW component (21^{o}), PGA = 0.156 g;
- Kobe, 1995, Kobe University record, NS component (90^{o}), PGA = 0.310 g.

As expected from the indications of sections 5.1 and 5.2, the largest maximum displacements (shown in Fig. 6), accelerations (Fig. 7) and interstorey drift angles (Fig. 8, where θ_j represents the angle between the (j − 1)-th and the j-th storey) are those developed by the SPD system, whilst the smallest ones are those developed by the MPD system (with R05 system providing intermediate performances). In detail:

- for all three damping systems considered, maximum displacement (acceleration) shows a smooth progressive rise from the bottom to the top of the structure[2]. For the three inputs here described, the top-storey displacements (accelerations) of the SPD system lie in the range between 35 and 65 mm ($4.0 \div 7.0$ m/sec^2), while those of the MPD system lie between 10 and 25 mm ($2.0 \div 2.5$ m/sec^2) and those of the R05 system between 20 and 30 mm ($2.5 \div 3.5$ m/sec^2);
- the absolute differences between maximum displacements (accelerations) of the SPD and MPD system increase from the bottom to the top of the structure, reaching their maximum value at the top itself. The differences being almost null at the first storey, and yet quite relevant at the second floor;
- the MPD system is able to reduce of more than 50% the maximum interstorey drift angles developed by the SPD system. The SPD system develops maximum values of the interstorey drift angle in the range between 0.40 and 0.75%, while the MPD system develops maximum values of the interstorey drift angle in the range between 0.10 and 0.25%.

Given the above systematic differences between the SPD and MPD system performances, it is quite surprising that the maximum forces developed by the dissipative devices of both MPD and SPD systems are comparable in size. As illustrative examples, for the El Centro record, the maximum force developed through dampers is 150 kN for the MPD system and 172 kN for the SPD one. For the Taft record, the maximum force developed through dampers is 88 kN for the MPD system and 84 kN for the SPD one. For the Kobe record, the maximum force developed through dampers is 117 kN for the MPD system and 93 kN for the SPD one. The distribution of the damper forces throughout the height of the structure is the opposite for the two systems: the MPD system transmits the largest dissipative force at the top of the structure, whilst the SPD system transmits the largest dissipative force at the bottom of the structure. With reference to the nomenclature of dampers of Fig. 9, Table 1 gives in detail the forces developed by the dampers at each storey, as obtained for the three earthquake inputs of above.

Fig. 10 shows the sum of the maximum forces developed in all dampers added to the structure for twenty earthquake ground motions (including El Centro 1940, Taft 1952 and Kobe 1995 records). In all cases, the total force developed through all dampers of the MPD system is again comparable with that of the SPD system. These results indicate that the better dissipative performances of the MPD system as compared to those of the SPD one do not come at the expense of larger damper forces.

Fig. 11 represents, for El Centro 1940, Taft 1952 and Kobe 1995 records, at each generic j-th storey: (a) the column shears applied to the "superstructure" resting over the floor $j-1$ (ensemble of floors j through N, considered as a free body) and (b) the "global" horizontal forces (column shears + forces transmitted through the damping devices) applied to the "superstructure". The MPD system leads to both column shears and "global" horizontal forces which are, at each storey, roughly one half of those given by the SPD system. This is a fundamental result that allows to claim that the MPD system has an intrinsically smaller response to earthquake excitation than that of the SPD system. MPD system does not only reduce the shear forces induced by the earthquake ground motions in the columns but indeed it reduces the overall earthquake-induced shears.

[2] The 3rd and 4th floor displacements (accelerations) are very similar due to the high lateral stiffness of the vertical members connecting the attic and the roof.

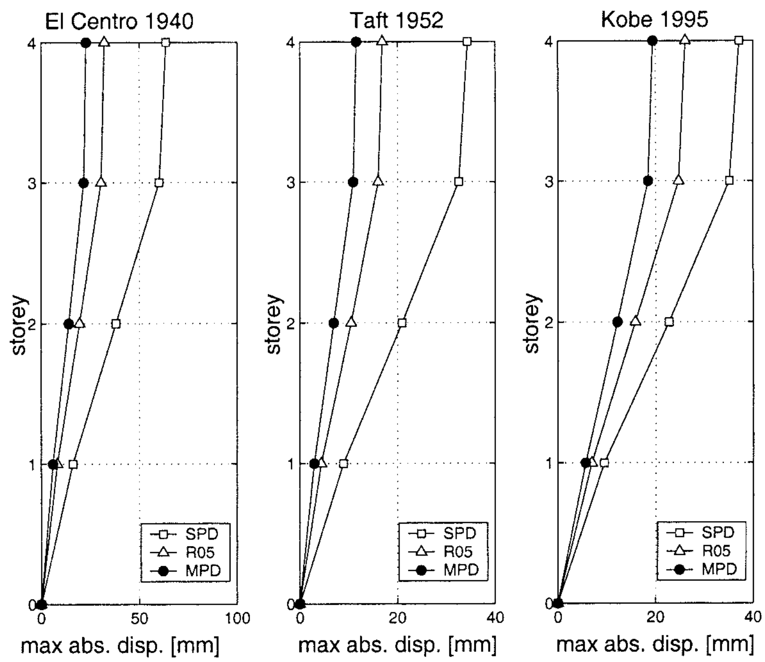

Fig. 6 Maximum frame displacements developed at each storey for the three earthquakes considered

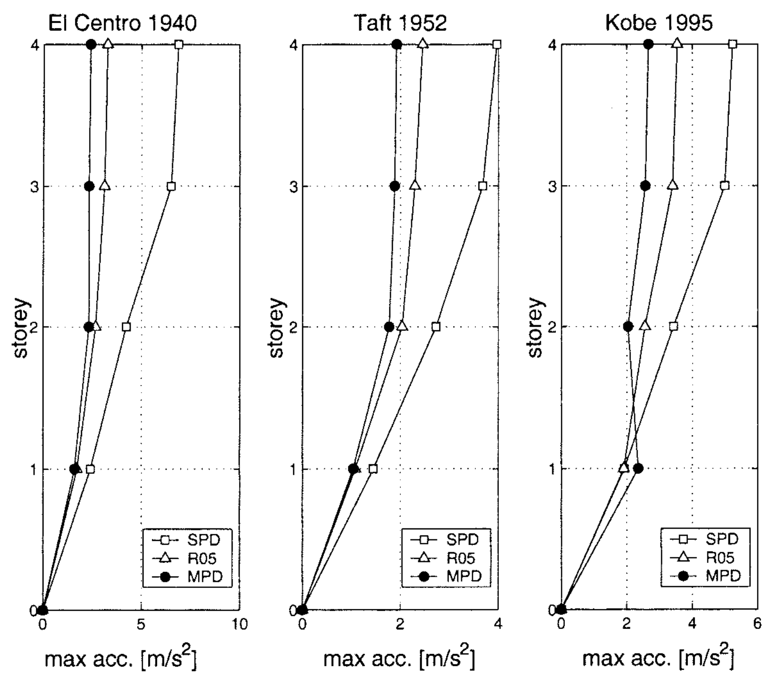

Fig. 7 Maximum accelerations developed at each storey for the three earthquakes considered

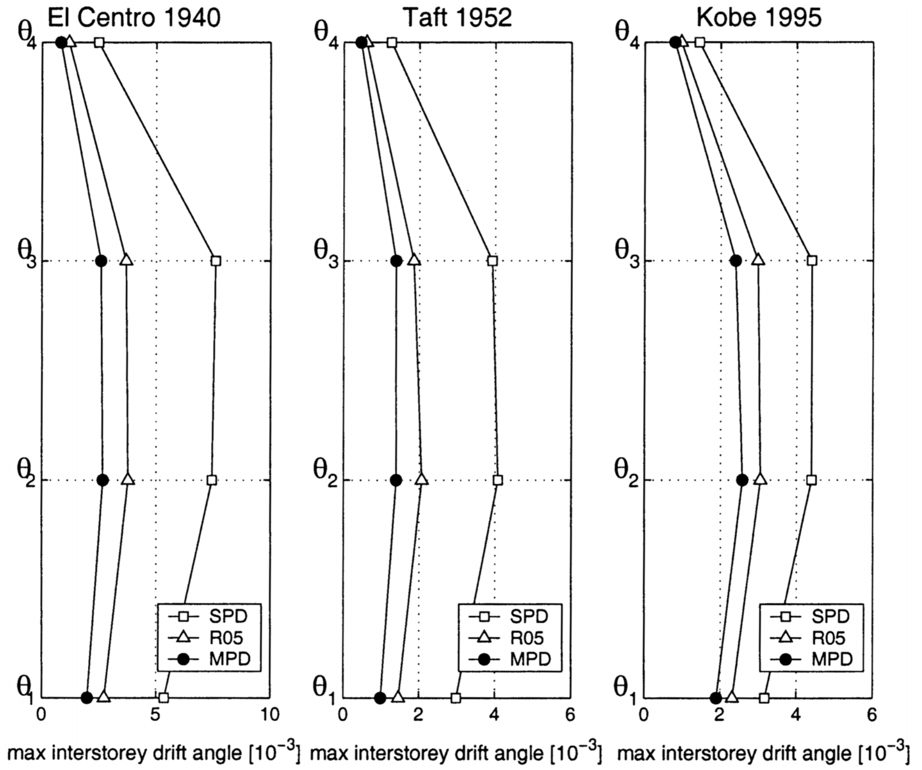

Fig. 8 Maximum interstorey drift angles developed for the three earthquakes considered

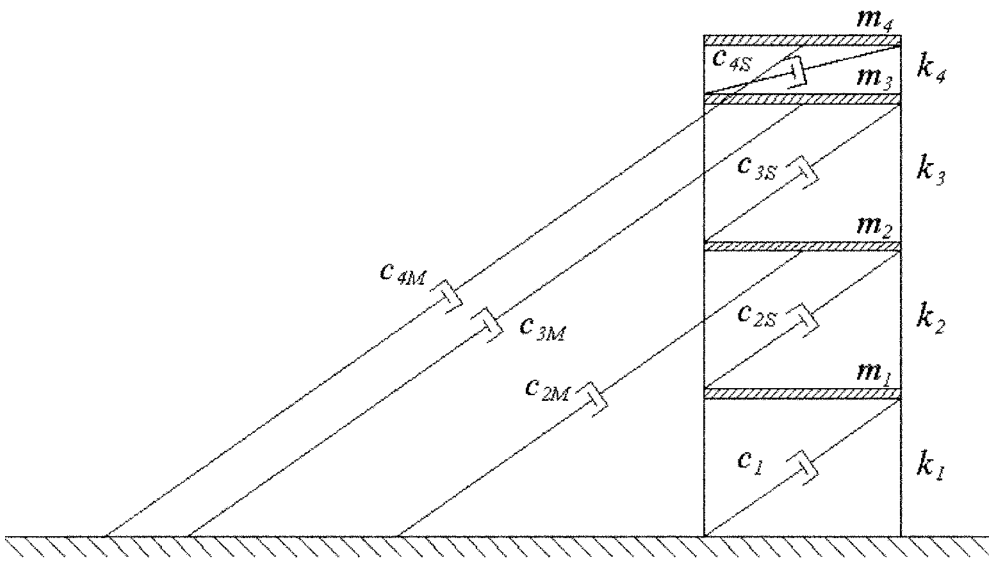

Fig. 9 Nomenclature of dampers for the frame considered

Table 1 Maximum forces [kN] developed through the dampers of MPD and SPD systems under the three earthquakes considered

	Damper	MPD system	SPD system
El Centro 1940	C1	63	172
	C2S	0	153
	C3S	0	107
	C4S	0	48
	C2M	128	0
	C3M	150	0
	C4M	120	0
	total	461	481
Taft 1952	C1	42	84
	C2S	0	76
	C3S	0	59
	C4S	0	27
	C2M	81	0
	C3M	88	0
	C4M	71	0
	total	281	245
Kobe 1995	C1	58	93
	C2S	0	82
	C3S	0	64
	C4S	0	30
	C2M	99	0
	C3M	117	0
	C4M	96	0
	total	370	268

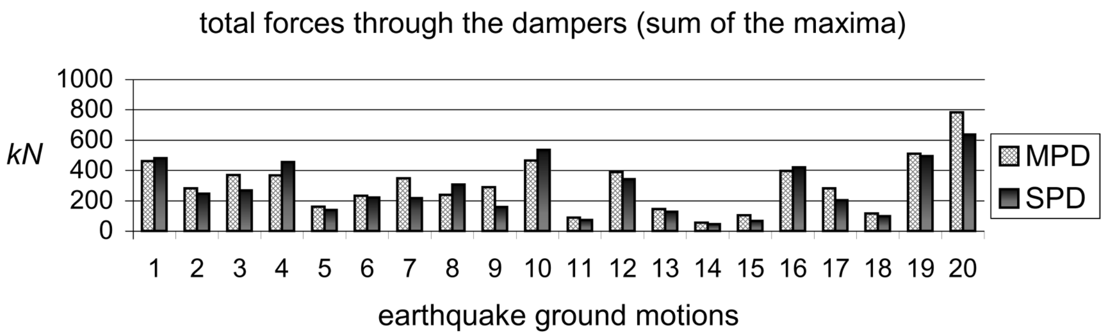

Fig. 10 Maximum total forces developed through the dampers under twenty earthquake records

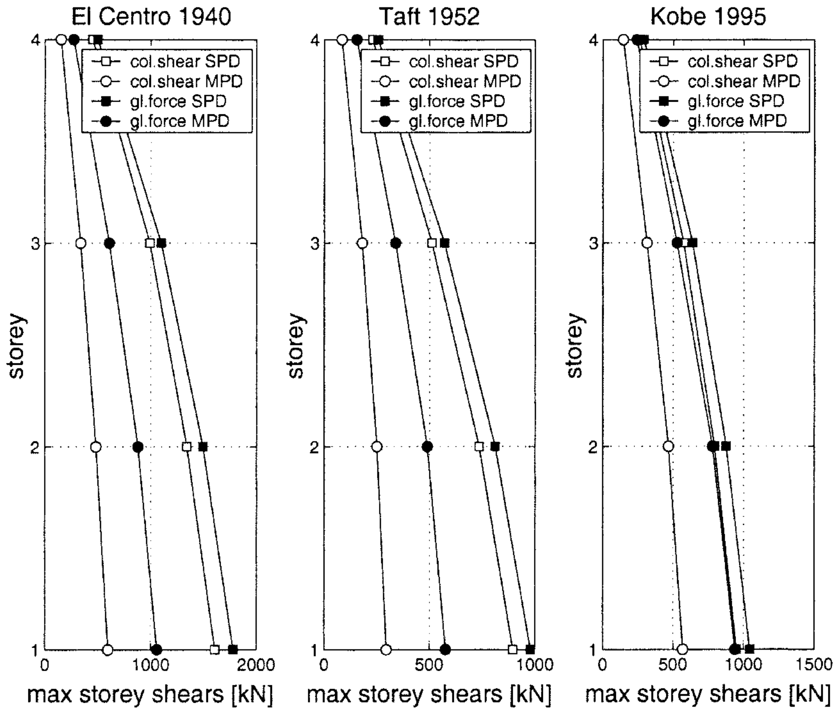

Fig. 11 Maximum column shears and "global" horizontal forces developed at each storey for the three earthquakes considered

6. Applicability of MPD systems

For the implementation in real structures of the long buckling-resistant braces necessary to create the MPD systems as per Fig. 2(a), the following technological solutions can be envisaged:

- use of the so-called "mega-braces" of Taylor Devices, already employed, even if not exactly following an MPD scheme, for the Chapultepec Tower (best known as Torre Major and shown in Fig. 12) in Mexico City. This bracing system has been successfully used to connect floors which are five storey apart.
- use of the so-called "unbonded braces" (Clark *et al.* 1999) of the Nippon Steel Corporation, already employed, even if not exactly following an MPD scheme, for the Osaka International Conference Centre (www.arup.com), shown in Fig. 13(a), and the retrofit of the Wallace F. Bennett Federal Building in Salt Lake City (Brown *et al.* 2001, www.aisc.org), shown in Fig. 13(b). This system has been successfully used to connect floors which are two storeys apart.
- use of prestressed steel cables coupled with silicon dampers, as proposed in the SPIDER European research project (Chiarugi *et al.* 2001). Researches regarding the effectiveness of this system (schematically represented in Fig. 14) are currently under development.

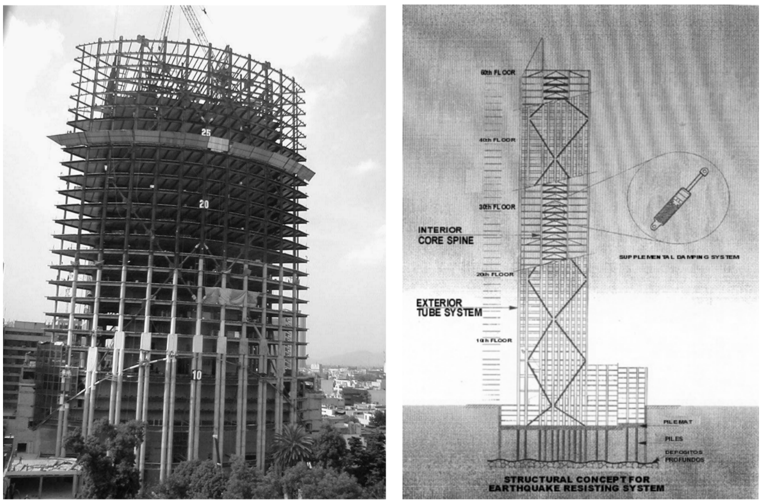

(a) (b)

Fig. 12 The Chapultepec Tower (best known as Torre Major) in Mexico City: (a) under construction and (b) schematic representation of the "mega-braces" of Taylor Devices

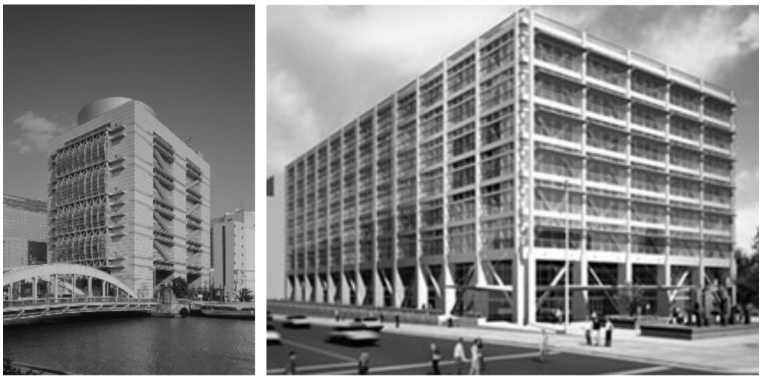

(a) (b)

Fig. 13 (a) Osaka International Conference Centre, (b) Wallace F. Bennett Federal Building

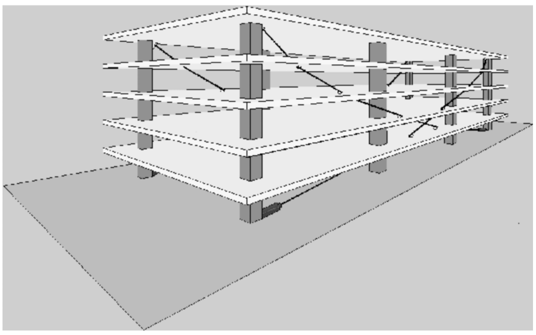

Fig. 14 Schematic representation of the damping cables of the SPIDER research project

7. Conclusions

In this paper, the definitions and the basic physical properties of the two limiting cases of Rayleigh damping - mass proportional damping (MPD) and stiffness proportional damping (SPD) - are briefly recalled. MPD systems and SPD systems correspond to two physically separated and actually independently implementable systems.

The advantages of the MPD system as applied to a concrete shear-type structure w.r.t. to other Rayleigh damping systems and in particular w.r.t the SPD system are here verified throughout numerical analyses. These analyses have been carried out against a specific 4-storey r.c. frame belonging to a structure designed in conformity with the Italian building code.

The MPD system is here identified as the Rayleigh damping system that minimises this structure's mean square response to a white noise stochastic input. On the other hand, use of the SPD system leads to the mean square response of this structure being maximised.

Consistently with these results, the modal damping ratio weighted average of the MPD system is computed to be about five times larger than that of the SPD system and the modal damping ratio weighted average of any Rayleigh system lies between these two limiting values.

Moreover, the response of the frame in question subjected to acceleration time-history simulations of 40 earthquakes applied to the base have confirmed the exceptional dissipative efficiency of the MPD system compared to the SPD one. It is also here presented how the better dissipative performances of the MPD system as compared to those of the SPD one do not come at the expense of larger damper forces.

Since SPD systems are characterised by the traditional interstorey damper placement and MPD systems by an innovative damper placement that sees dampers connecting each storey to a fixed point, the results here presented clearly indicate a new efficient way for inserting added viscous dampers in shear-type structures.

Acknowledgements

The authors are grateful to Dr. Philippe Duflot of Taylor Devices Europe (for kindly providing information regarding the application of "mega-braces" in the Chapultepec Tower) and to Prof. Stefano Sorace of University of Udine (for kindly allowing the inclusion of the picture representing the schematic functioning of the SPIDER dissipative bracing system).

References

Brown, P., Aiken, I.D. and Jafarzadeh, F.J. (2001), "Seismic Retrofit of the W. F. Bennett Federal building", *Modern Steel Construction.*

Chiarugi, A., Terenzi, G. and Sorace, S. (2001), "Metodo di progetto di dispositivi siliconici per l'isolamento alla base: applicazione a due casi sperimentali", Atti del 10º Convegno Nazionale ANIDIS, Potenza-Matera, Italy.

Chopra, A.K. (1995), *Dynamics of Structures, Theory and Applications to Earthquake Engineering*, Prentice Hall, Englewood Cliffs.

Clough, R.W. and Penzien, J. (1993), *Dynamics of Structures*, 2nd edition, McGraw-Hill International Editions, Civil Engineering Series, New York.

Contantinou, M.C. and Tadjbakhsh, I.G. (1983), "Optimum design of a first story damping system", *Comp.*

Struct., **17**(2), 305-310.

Crandall, S.H. and Mark, W.D. (1963), *Random Vibrations in Mechanical Systems*, Academic Press, New York and London.

De Silva, C.W. (1981), "An algorithm for the optimal design of passive vibration controllers for flexible systems", *J. Sound Vib.*, **75**(4), 495-502.

Hahn, G.D. and Sathiavageeswaran, K.R. (1992), "Effects of added-damper distribution on the seismic response of buildings", *Comp. Struct.*, **43**(5), 941-950.

Hart, G.C. and Wong, K. (2000), *Structural Dynamics for Structural Engineers*, John Wiley & Sons, New York.

Lopez Garcia, D. (2001), "A simple method for the design of optimal configurations in MDOF structures", *Earthquake Spectra*, **17**(3), 387-398.

Singh, M.P. and Moreschi, L.M. (2001), "Optimal seismic response control with dampers", *Earth. Eng. Struct. Dyn.*, **30**(4), 553-572.

Singh, M.P. and Moreschi, L.M. (2002), "Optimal placement of dampers for passive response control", *Earth. Eng. Struct. Dyn.*, **31**(4), 955-976.

Skalmierski, B. and Tylikowski, A. (1982), *Stochastic Processes in Dynamics*, Martinus Nijhoff Publishers, London or PWN/Polish scientific publishers, Warsawa.

Takewaki, I. (1997), "Optimal damper placement for minimum transfer functions", *Earth. Eng. Struct. Dyn.*, **26**, 1113-1124.

Takewaki, I. (1998), "Optimal damper positioning in beams for minimum dynamic compliance", *Comp. Meth. Appl. Mech. Eng.*, **156**, 363-373.

Takewaki, I. (1999), "Displacement-acceleration control via stiffness-damping collaboration", *Earth. Eng. Struct. Dyn.*, **28**(12), 1113-1124.

Takewaki, I. (2000), "Optimal damper placement for critical excitation", *Prob. Eng. Mech.*, **15**, 317-325.

Trombetti, T., Ceccoli, C. and Silvestri, S. (2001), "Mass proportional damping as a seismic design solution for an 18-storey concrete-core & steel-frame structure", *Proc. of the Speciality Conf. on "The Conceptual Approach to Structural Design"*, Singapore, August 2001.

Trombetti, T., Silvestri, S. and Ceccoli, C. (2002) "Inserting viscous dampers in shear-type structures: Analytical formulation and efficiency of MPD system", *Proc. of the Second Int. Conf. on Advances in Structural Engineering and Mechanics (ASEM'02),* Pusan, Korea, August 2002.

Trombetti, T., Silvestri, S. and Ceccoli, C. (2002), "Added viscous dampers in shear-type structures: the effectiveness of mass proportional damping", *N. T. n^o 58.* DISTART, Università di Bologna, Italy.

Zhang, R.H. and Soong, T.T. (1992), "Seismic design of viscoelastic dampers for structural applications", *J. Str. Eng.*, ASCE, **118**(5), 1375-1392.

http://nisee.berkeley.edu/prosys/applications.html

http://www.arup.com/dyna/applications/seismic/seismic.htm

http://www.aisc.org/Content/ContentGroups/Modern_Steel_Construction3/August_2001/0108_03_seismicretrofit.pdf